Bayesian inference of the critical endpoint in 2+1-flavor system from holographic QCD

Liqiang Zhu

Collaborated with Xun Chen, Kai Zhou, Hanzhong Zhang and Mei Huang

Phys.Rev.D 112 (2025) 2, 026019

November 2, 2025

第4届全国核物理及核数据中的
机器学习应用研讨会

華中師範大學
CENTRAL CHINA NORMAL UNIVERSITY

Outline

1. Introduction and motivation

2. Einstein-Maxwell-Dilaton (EMD) model

3. Application of EMD model: Bayesian location of the QCD Critical Endpoint

4. Summary

Introduction and motivation

Unraveling the Fundamental Composition and Interactions of Matter

Exploring the Nature of Strong Interactions

Simulating Extreme Conditions of the Early Universe

Exploring Mechanisms of Phase Transitions in Matter

Non-perturbative methods:

Lattice simulation

Holography: gauge/gravity dual or

AdS/QCD correspondence

Other low energy effective model. eg.

HRG, NJL , PNJL, fRG, ...

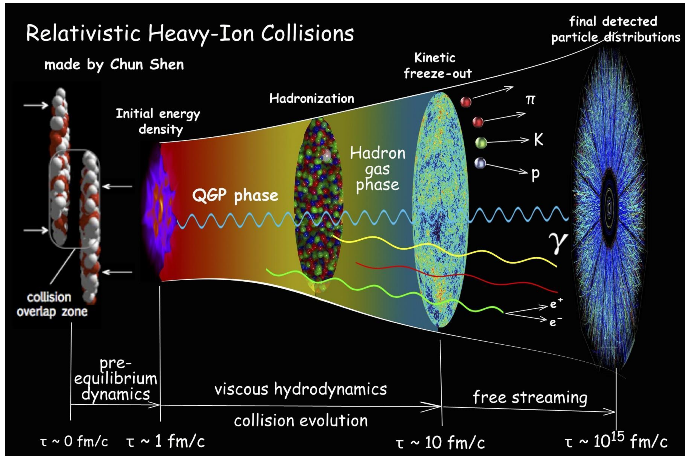

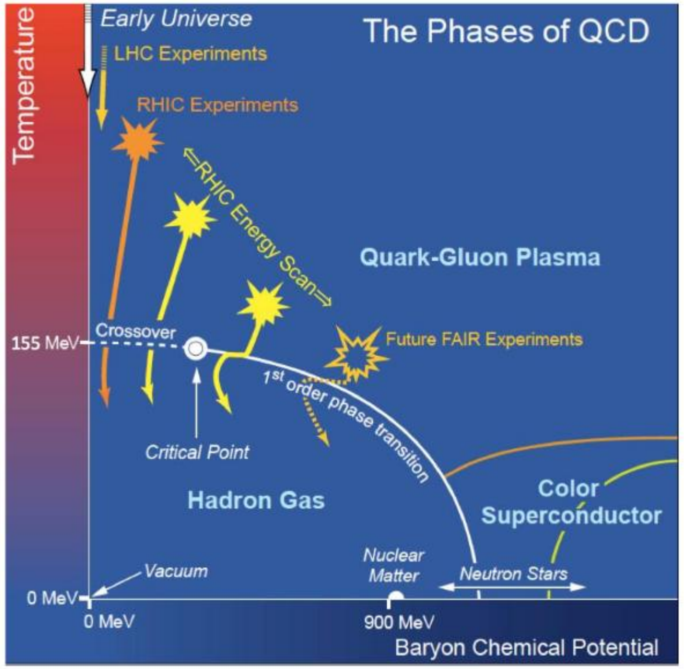

Einstein-Maxwell-Dilaton (EMD) model

The Einstein-Maxwell-dilaton(EMD) action ：

$$S_b=\frac{1}{16\pi G_5}\int d^5x\sqrt{-g^s}\,e^{-2\phi_s}\left[R_s-\frac{f_s(\phi_s)}{4}F^2+4\partial_\mu\phi_s\partial^\mu\phi_s-V_s(\phi_s)\right]\qquad f(z)=e^{cz^2-A(z)+k}$$

chemical potential **dilaton field: breaking conformal invariance**

The metric :

$$ds^2=\frac{L^2e^{2A(z)}}{z^2}\left[-g(z)dt^2+\frac{dz^2}{g(z)}+d\vec{x}^2\right]\quad A(z)=d\ln(az^2+1)+d\ln(bz^4+1)$$

Dilaton field :

$$\phi'(z)=\sqrt{6(A'^2-A''-2A'/z)}$$

Xun Chen, Mei Huang,Flavor dependent critical endpoint from holographic QCD through machine learning, JHEP 02 (2025) 123.

Einstein-Maxwell-Dilaton (EMD) model

The Hawking temperature and entropy :

$$T = \frac{z_h^3 e^{-3A(z_h)}}{4\pi \int_0^{z_h} dy\, y^3 e^{-3A(y)}} \left[1 + \frac{2c\mu^2 e^k \left(e^{-cz_h^2} \int_0^{z_h} dy\, y^3 e^{-3A(y)} - \int_0^{z_h} dy\, y^3 e^{-3A(y)}\, e^{-cy^2} \right)}{(1 - e^{-cz_h^2})^2} \right]$$

$$S = \frac{e^{3A(z_h)}}{4G_5 z_h^3}$$

The squared speed of sound :

$$C_s^2 = \frac{S}{T\left(\frac{\partial S}{\partial T}\right)_\mu + \mu\left(\frac{\partial \rho}{\partial T}\right)_\mu}$$

The second-order baryon susceptibility :

$$\chi_2^B = \frac{1}{T^2} \frac{\partial \rho}{\partial \mu}$$

Bayesian Inference Process

Parameters
$\boldsymbol{\theta} = \boldsymbol{\theta}(a, b, c, d, k, G_5)$

Latin Hypercube

EMD MODEL

Gaussian process emulator

Evidence : lattice results of $S/T^3, \chi_2^B, C_s^2$

$$P(\text{data}|\theta) = \prod_i \frac{1}{\sqrt{2}\sigma_i} e^{-\frac{\left(y_i(\theta) - y_i^{\text{exp}}\right)^2}{2\sigma_i^2}}$$

$$P(\theta|\text{data}) \propto P(\text{data}|\theta) P(\theta)$$

σ_i : Experimental error and Gaussian Emulator error

MCMC

Posterior $P(\theta|\text{data})$

The prior to lattice data with EMD model

Case 1 : S/T^3 and χ_2^B as Prior

Case 2 : S/T^3 , χ_2^B and C_S^2 as Prior

Prior		
Parameter	min	max
a	0.110	0.310
b	0.005	0.031
c	-0.280	-0.205
d	-0.240	-0.110
k	-0.910	-0.770
G_5	0.375	0.430

300 sets of θ for prior

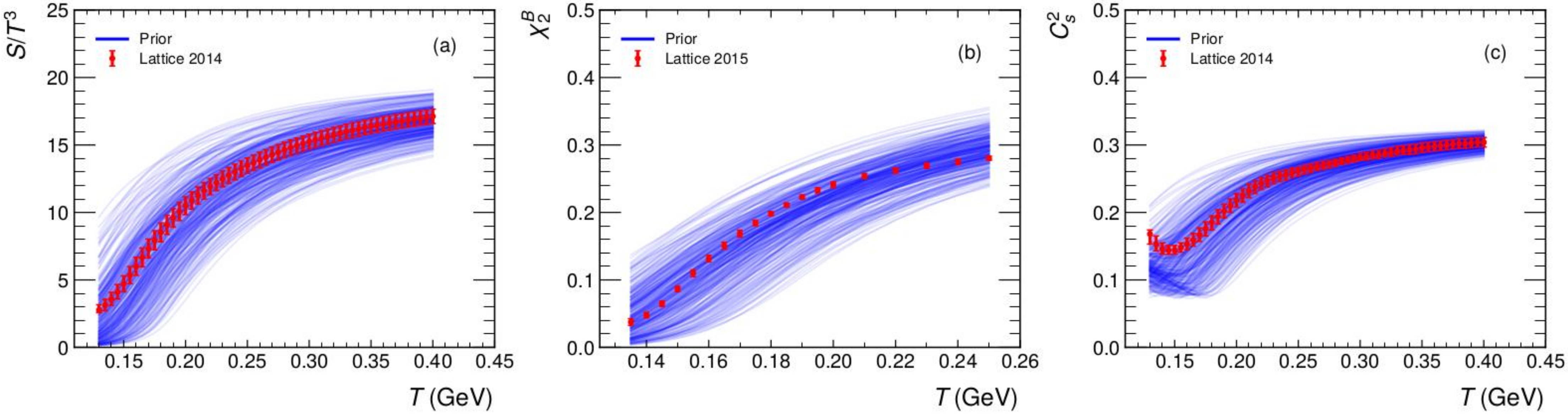

HotQCD Collaboration,Equation of state in (2+1)-flavor QCD,Phys.Rev.D 90 (2014) 094503

A. Bazavov, H. -T. Ding et al. , The QCD Equation of State to $O\mu_B^6$ from Lattice QCD, Phys.Rev.D 95 (2017) 5, 054504

Posterior distributions of the EMD model parameters

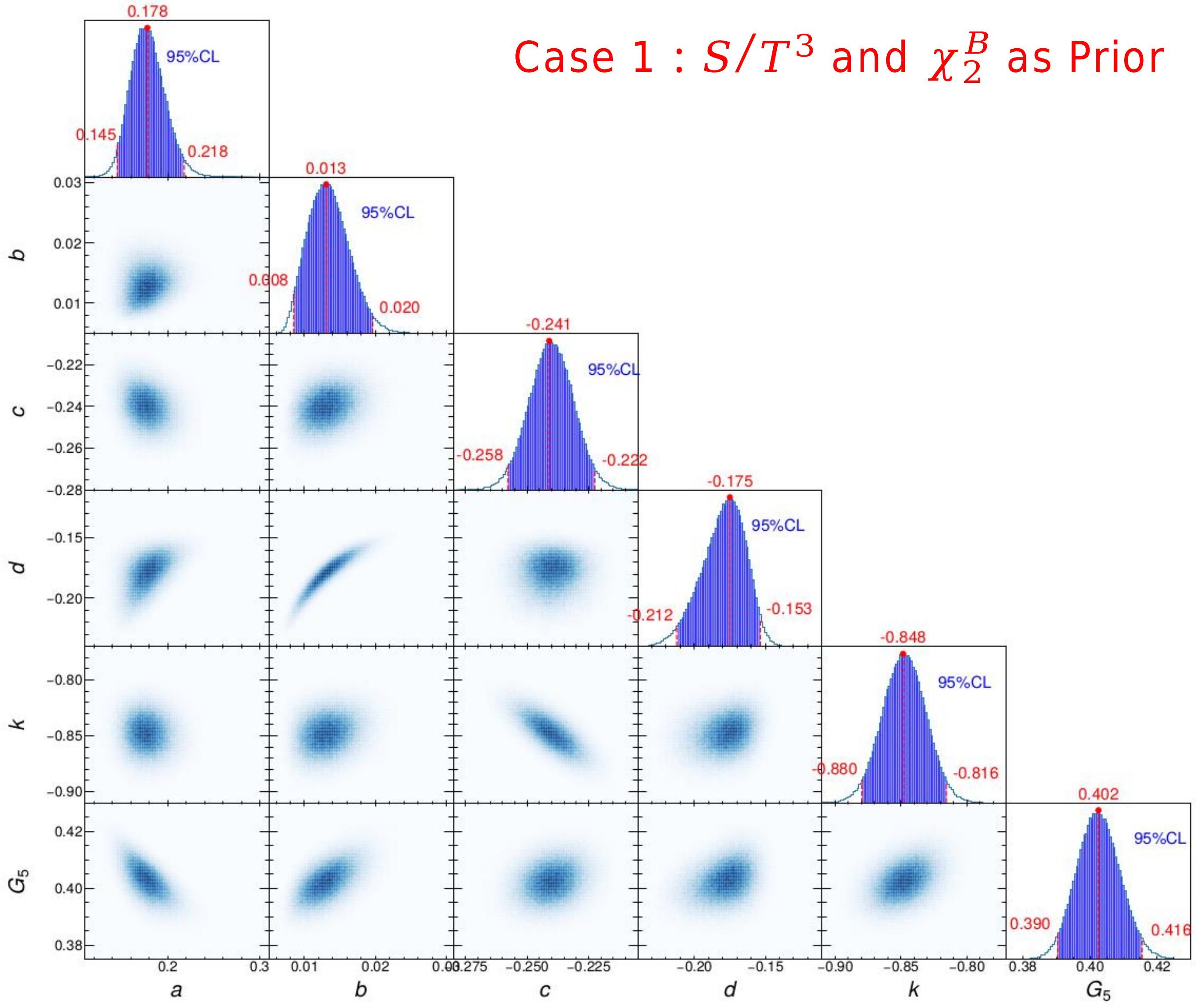

Case 1 : S/T^3 and χ_2^B as Prior

Posterior distributions of the model parameters(diagonal panels), together with their correlations (off-diagonal panels).

Maximum a posteriori (MAP)

Posterior 95% CL			
Parameter	min	max	MAP
a	0.145	0.218	0.178
b	0.008	0.020	0.013
c	-0.258	-0.222	-0.241
d	-0.212	-0.153	-0.175
k	-0.880	-0.816	-0.848
G_5	0.390	0.416	0.402

Posterior distributions of the model parameters

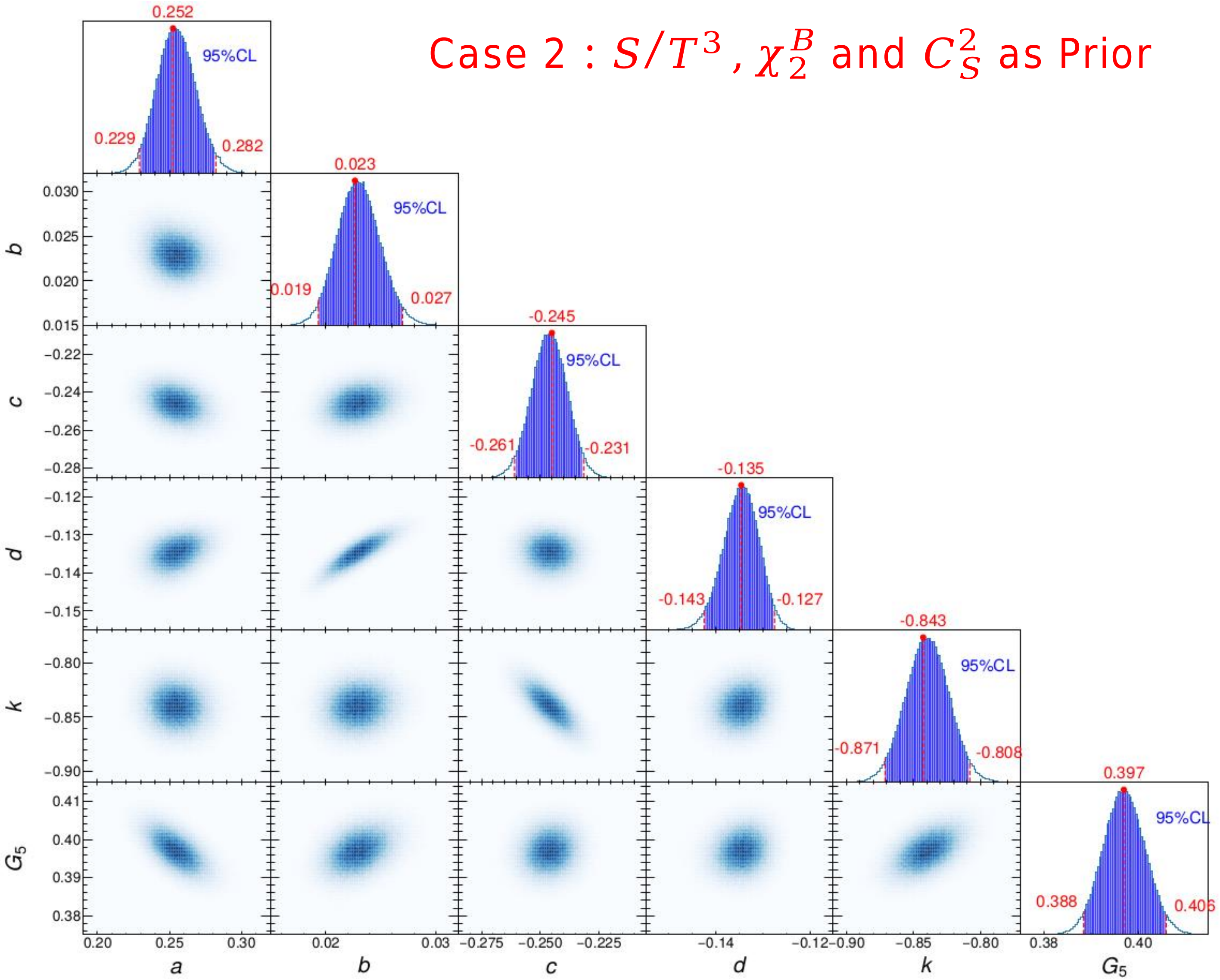

Case 2 : S/T^3 , χ_2^B and C_S^2 as Prior

Posterior distributions of the model parameters(diagonal panels), together with their correlations (off-diagonal panels).

Maximum a posteriori (MAP)

Posterior 95% CL			
Parameter	min	max	MAP
a	0.229	0.282	0.252
b	0.019	0.027	0.023
c	-0.261	-0.231	-0.246
d	-0.143	-0.127	-0.135
k	-0.871	-0.808	-0.843
G_5	0.388	0.406	0.397

Prior selection and thermodynamic consistency—Case 1 VS Case 2

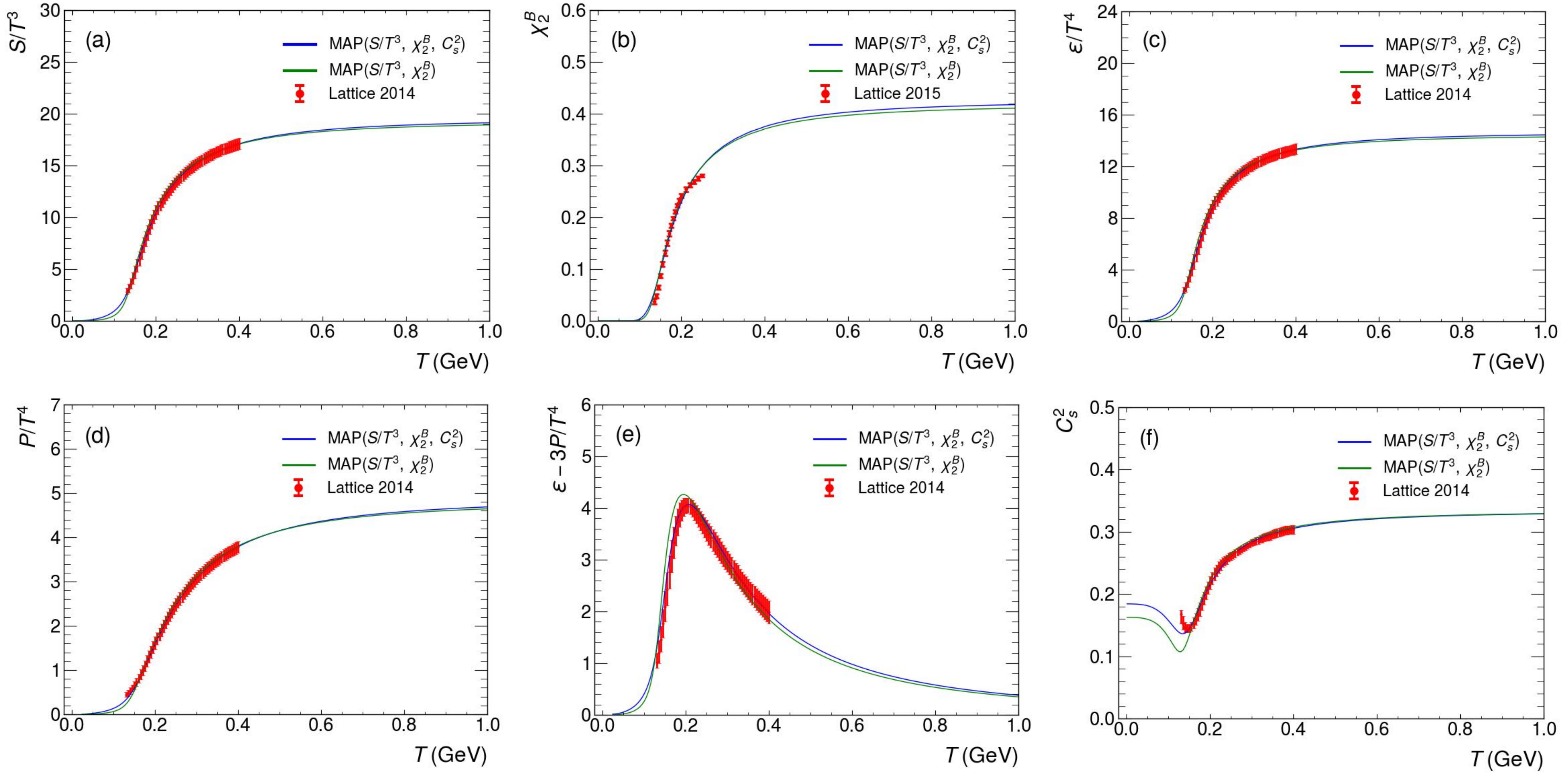

Prior selection and thermodynamic consistency—Case 1 VS Case 2

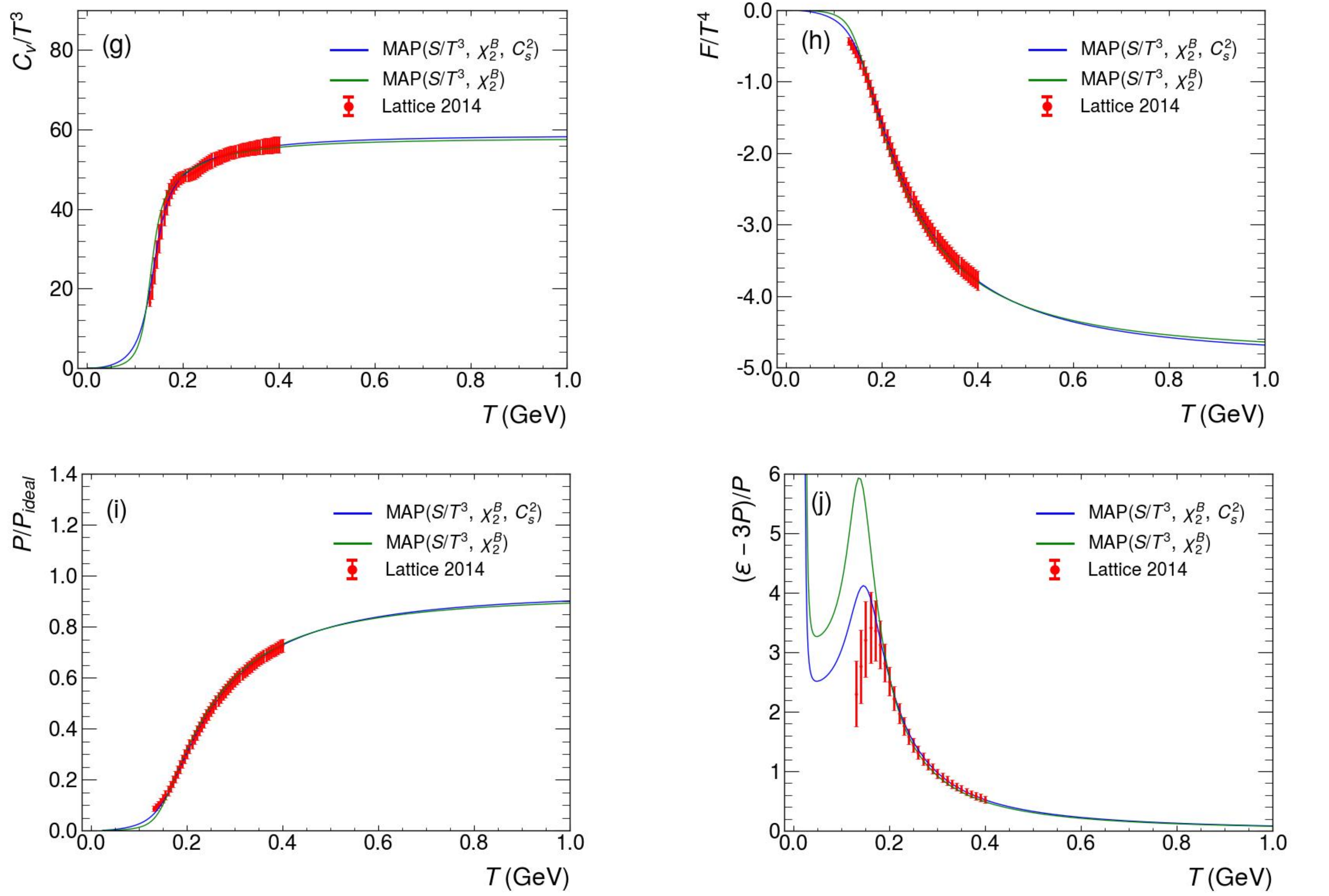

The posteiror comparison to HRG ,HTL and Lattice—Case 2

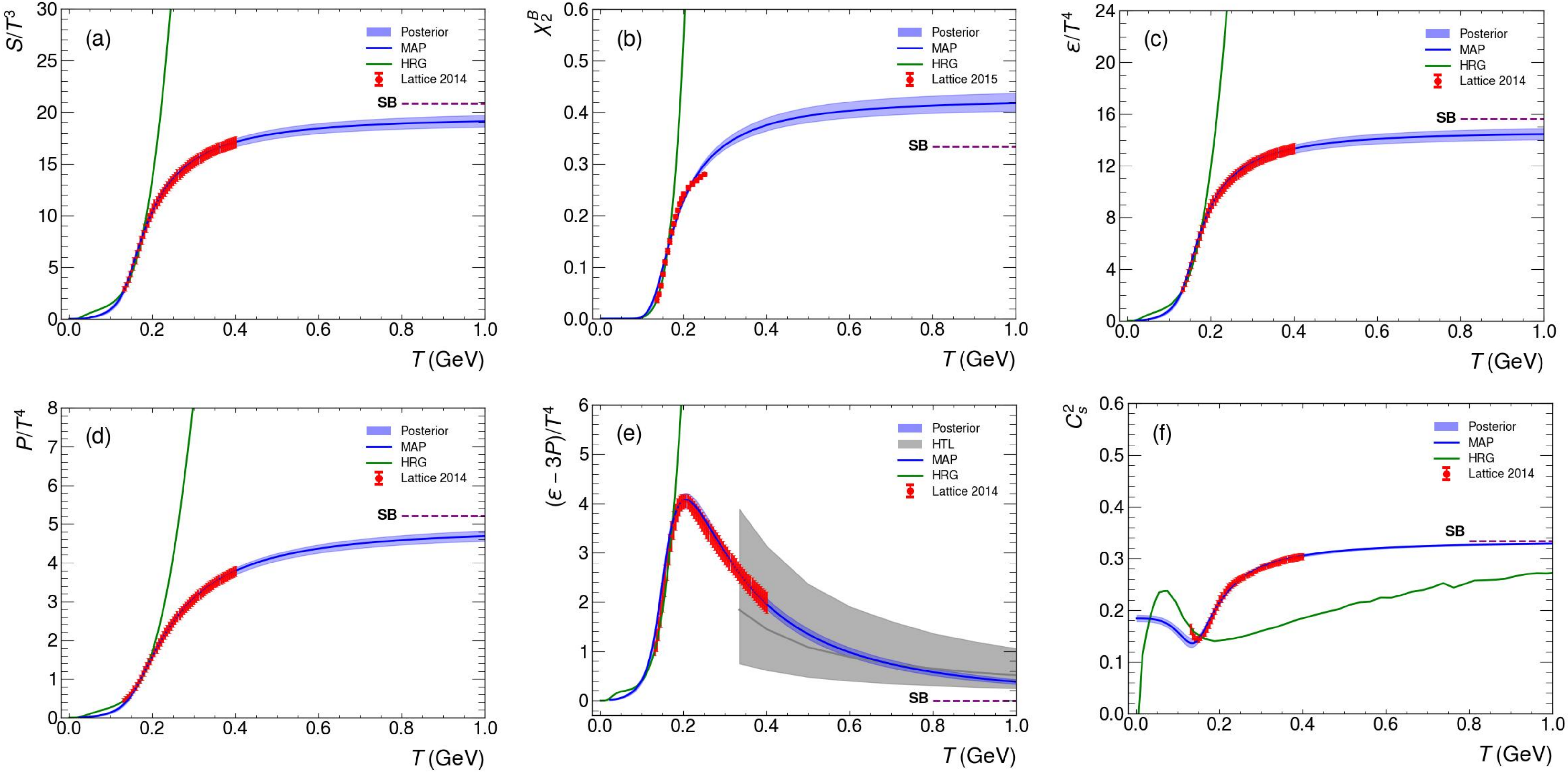

The posteiror comparison to HRG ,HTL, and Lattice—Case 2

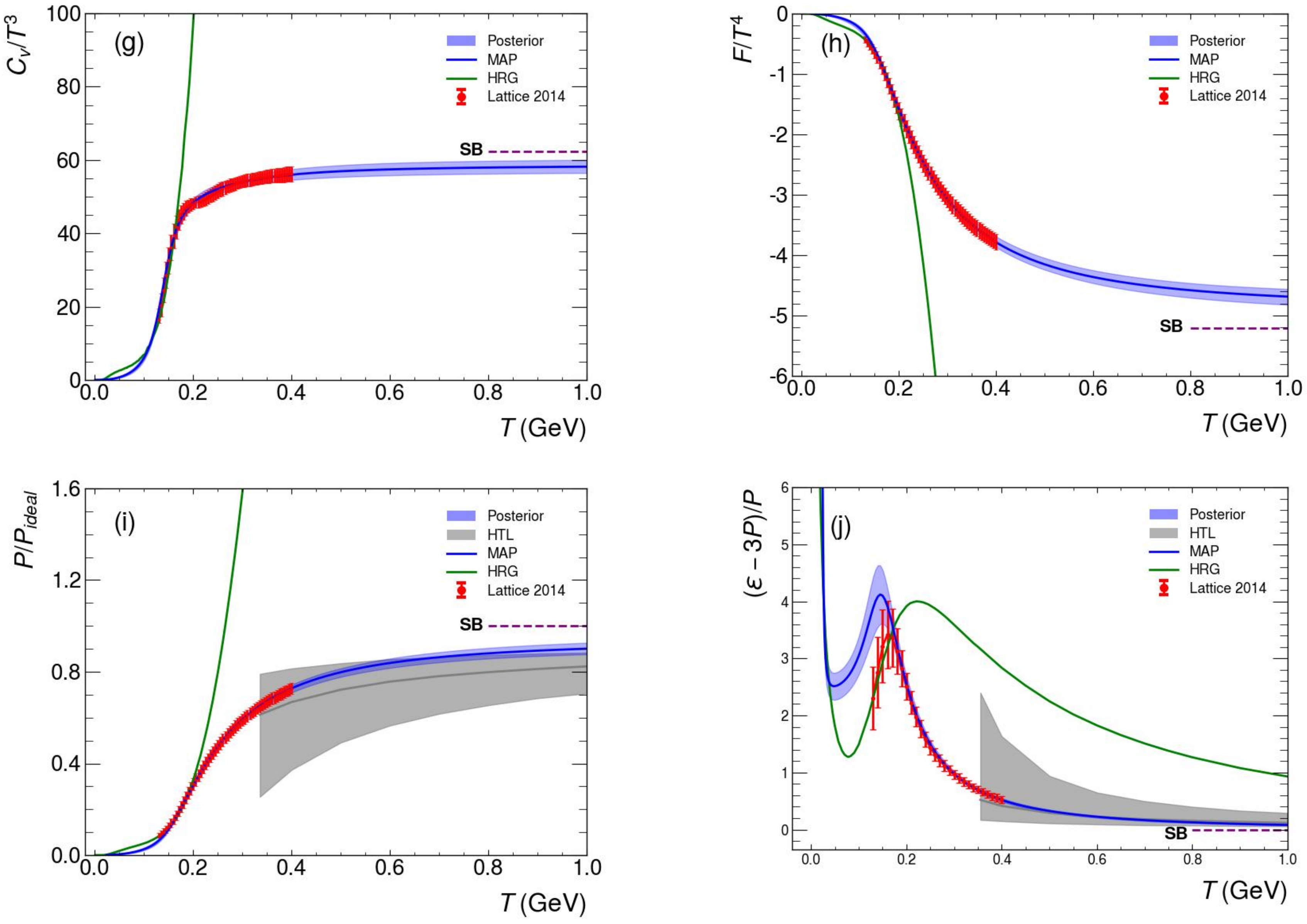

Bayesian location of the CEP—Case 1 VS Case 2

Case 1

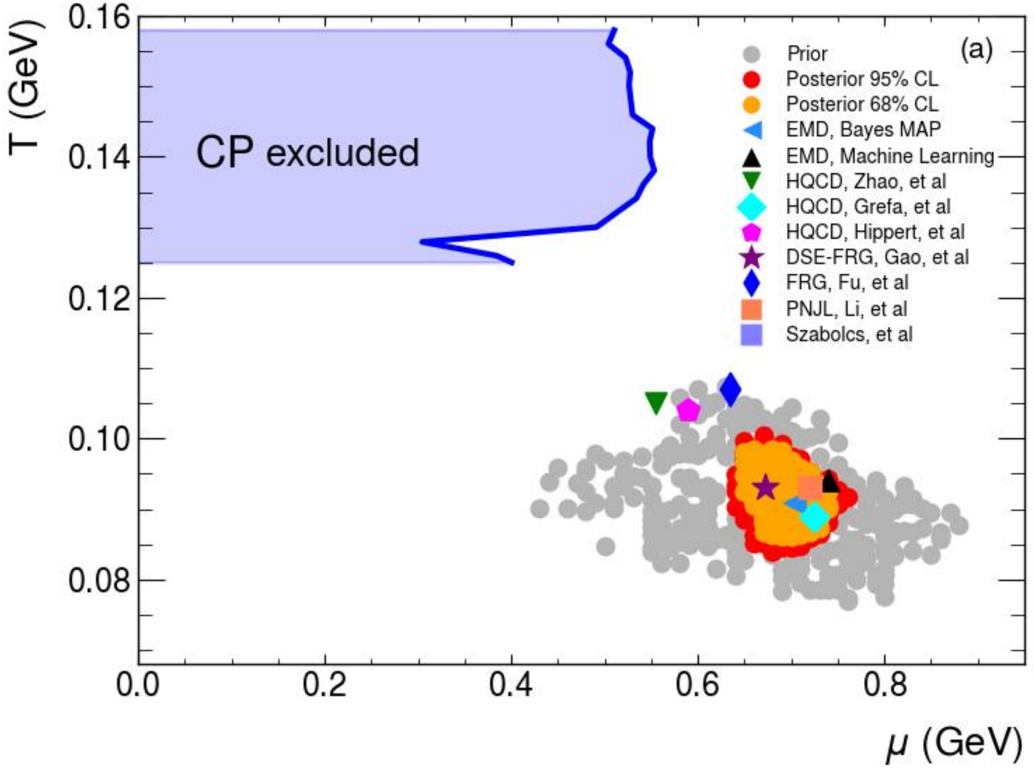

$$(T_c, \mu_B^c)_{\mathrm{MAP}} = (0.0909, 0.704)\ \mathrm{GeV}$$

$$(T_c, \mu_B^c)_{68\%} = (0.0846 - 0.0985, 0.65 - 0.74)\ \mathrm{GeV}$$

$$(T_c, \mu_B^c)_{95\%} = (0.0839 - 0.1003, 0.64 - 0.76)\ \mathrm{GeV}$$

Case 2

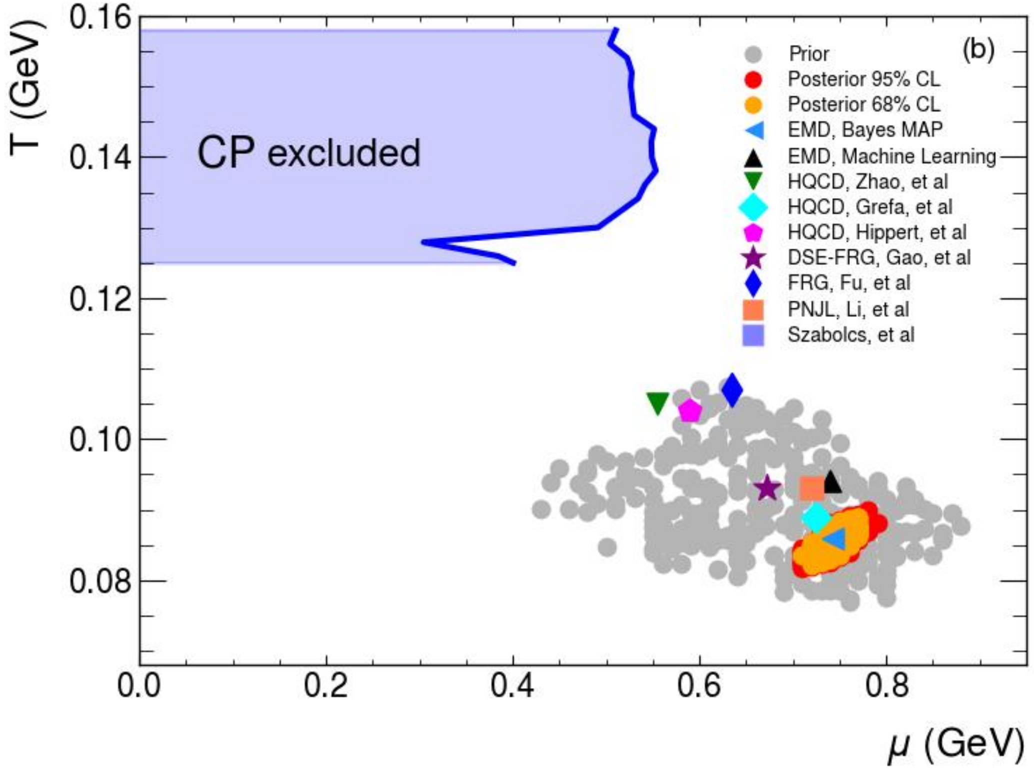

$$(T_c, \mu_B^c)_{\mathrm{MAP}} = (0.0859, 0.742)\ \mathrm{GeV}$$

$$(T_c, \mu_B^c)_{68\%} = (0.0820 - 0.0889, 0.71 - 0.77)\ \mathrm{GeV}$$

$$(T_c, \mu_B^c)_{95\%} = (0.0816 - 0.0898, 0.71 - 0.79)\ \mathrm{GeV}$$

Summary

We present a prediction of the critical endpoint location in the high-density phase of strongly interacting matter, which is obtained by using Bayesian inference together with lattice QCD data at zero chemical potential and the EMD model.

entropy, susceptibility as prior:

68% Confidence Interval (T_c: 0.0861 GeV~0.0985 GeV , μ_B^c: $0.65\ GeV$~0.74 GeV)

95% Confidence Interval (T_c: 0.0839 GeV~0.1003 GeV , μ_B^c: $0.64\ GeV$~0.76 GeV)

entropy, susceptibility, square of the speed of sound as prior:

68% Confidence Interval (T_c: 0.0822 GeV~0.0889 GeV , μ_B^c: $0.71\ GeV$~0.77 GeV)

95% Confidence Interval (T_c: 0.0817 GeV~0.0898 GeV , μ_B^c: $0.71\ GeV$~0.79 GeV)

Thank You !